AN INVESTIGATION OF THE DYNAMICALLY INDUCED STRESSES IN A TYPICAL HIGHWAY BRIDGE

James C. Longley, M.S.
The University of Connecticut, June 1966

Report No. JHR 66-4 July 1966

Research carried out through the Joint Highway Research Council of the University of Connecticut and the Connecticut Department of Highways. Paper written as thesis requirement for M.S. under guidance of Professor E. Russell Johnston, Jr.

TABLE OF CONTENTS

TABLE OF CONTENTS CONTINUED

LIST OF ILLUSTRATIONS

I

INTRODUCTION

In the course of a study of bridge deck deterioration conducted by the Civil Engineering Department at the University of Connecticut for the Connecticut State Highway Department during the summer of 1965, some preliminary investigations were made of the effect of vehicle induced vibration on the cracking tendancies of the concrete decks. This preliminary investigation consisted of approximate measurements of the mid-span deflections of several bridges and a correlation of the human sensation of vibration, generally initiated by a large truck, with the overall condition of the deck. The results of this work indicated that further study was needed.

The basic question centered around the magnitude of tensile stresses in the bridge decks, caused by the negative moment present during the upward deflection, due to free vibrations resulting from a vehicle's passage. The inherently low tensile strength of concrete, coupled with a reduction of strength due to fatigue, pointed to the possibility of initiation of dynamically induced cracks. Once cracked, the deck could be subjected to increased weathering effects or abrasion which would hasten deterioration.

To facilitate an analytical solution to the problem an electrical circuit was designed for the Electronics Associates Incorporated PACE 231 analog computer in the University of Connecticut's Computer Center. This circuit simulates a dampened, lumped mass, simple span bridge under the

influence of a single wheeled vehicle consisting of a sprung mass and an unsprung mass with an equivalent viscous damping shock absorber. Using this analogy a typical bridge was studied to determine the influence of vehicle speed and the presence of variations in the height of the approach slab on the order of magnitude of the resulting tensile stresses.

II

PRELIMINARY INVESTIGATION

While undertaking a broad study of the deterioration of bridge decks for the Connecticut State Highway Department during the summer of 1965, some attention was focused on the problem of vibration induced cracks. When a highway bridge is transversed by a sprung vehicle, the two interact with each other in such a way as to introduce vibration to the bridge. Once the vehicle leaves the bridge it continues to oscillate in free vibration. In this mode the bridge deflection is both above and below its unloaded position. When the deflection is upward, the concrete will be placed in tension.* It was felt that the transverse cracking of the bridge decks might have been a result of this tension produced during free vibration.

First impressions obtained from a cursory examination of several bridges, indicated an apparently large amplitude of vibrations due to the passage of large trucks. In that the human body is quite sensitive to this type of vibration it was felt that a closer determination of the order of magnitude of the deflections would be wise.

Several bridges were studied to determine the magnitude of the dynamic deflections. In order to measure the deflection several methods were tried with varying degrees of success. The first method involved the use of a steel pipe, fitted with couplings for packing purposes. The pipe was dropped to the roadway beneath the bridge and the deflec-

* The deadload stress in the concrete is zero.

tions were indicated by the extent of the mark on the pipe, produced by a pencil held firmly on the side of the bridge. This method was used on several simple span bridges to measure total centerline deflections of about 1/8 inch.

It became evident that the measuring method left something to be desired, so the next step was the use of a long wire fastened to a spring, which in turn was fastened to the bridge. The free end of the wire was weighted to facilitate handling when dropping it from the bridge to the surface below, where it was anchored securely. Deflection could then be measured by finding the maximum movement between the top end of the wire and the bridge. Use of this equipment on several hung span bridges resulted in measured total deflections between 1/8 inch and 1/6 inch at the centerline of the hung span. In each case it was difficult to differentiate between deflections above and below the unloaded position.

On each of the more than 100 bridges observed, a classification of the relative vibrational characteristics was made by the team of observers. This classification consisted of a consensus as to whether the bridge was "bouncy" or "not bouncy". It should be pointed out that the physiological effects of vibration are not an objective determination. The human body is more sensitive to certain frequencies and amplitudes of vibration than to others. Generally speaking, low frequencies and large amplitudes are most noticeable (1,2). * Evaluation of the observed characteristics at the conclusion of the study indicated the following:

1. A higher percentage of hung and continuous spans were bouncy as compared to simple spans.

* Numbers in parenthesis refer to references included in the List of References.

2. The longer a span was the higher the tendancy toward larger total dynamic deflection.
    a. Plate girders showed a greater tendancy to be "bouncy" than other types. No doubt, this is because plate girders and hung or continuous spans are required for the longer bridges. As the length of a beam increases its frequency decreases and its amplitude increases, thus becoming more noticeable.
3. There was a higher percentage of numerous transverse cracks and random cracks on bouncy bridges.
4. The over-all condition was independent of bouncyness.

The results of this preliminary investigation were considered insufficient as convincing evidence of the vibrational effects, but they did indicate that an analytical solution would be desirable.

III

BASIC EQUATIONS

Transverse Vibration of a Beam

To evolve the basic equation required for preparation of an electrical analogy we shall consider a beam in which the thickness is small compared to the length. A differential element of the beam is shown below.

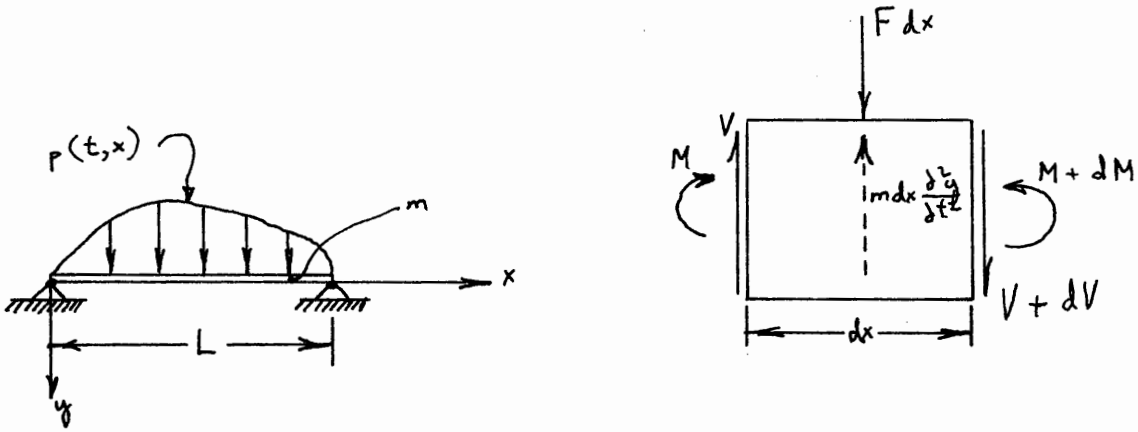

Figure 1. A Beam and Differential Element

The mass per unit length is denoted by m; and the load intensity, which is a function of distance along the beam and time, is denoted by p. The bending moment M and the shear V, are both positive in the direction shown. When the positive load is taken in the same direction as the positive y axis, the total load intensity is

$$w = F(t,x) - m\frac{\partial^2 y}{\partial t^2} \quad \ldots\ldots\ldots\ldots\ldots\ldots\ldots\ldots (1).$$

The relationship between deflection, moment, and load is

$$M = -EI \frac{\partial^2 y}{\partial x^2} \quad \ldots\ldots\ldots\ldots\ldots\ldots\ldots\ldots\ldots (2).$$

$$-w = \frac{\partial^2 M}{\partial x^2} = -EI \frac{\partial^4 y}{\partial x^4} \quad \ldots\ldots\ldots\ldots\ldots\ldots\ldots (3).$$

where EI, which is assumed constant along the length of the span, is the rigidity of the beam. Combining equations (1) and (3) results in the equation of motion for the transverse vibration of the beam.

$$EI \frac{\partial^4 y}{\partial x^4} + m \frac{\partial^2 y}{\partial t^2} = F(t,x) \quad \ldots\ldots\ldots\ldots\ldots (4).$$

If an equivalent viscous damping is included, equation (4) becomes

$$EI \frac{\partial^4 y}{\partial x^4} + m \frac{\partial^2 y}{\partial t^2} + C \frac{\partial y}{\partial t} = F(t,x) \quad \ldots\ldots\ldots\ldots (5).$$

For this derivation the effects of shear deformation and of the rotation of the element have been neglected. However, when considering a slender beam these effects are not important and will be neglected here.

Dynamic Equilibrium of the Vehicle

For the purposes of this study the vehicle to be considered is represented as shown below.

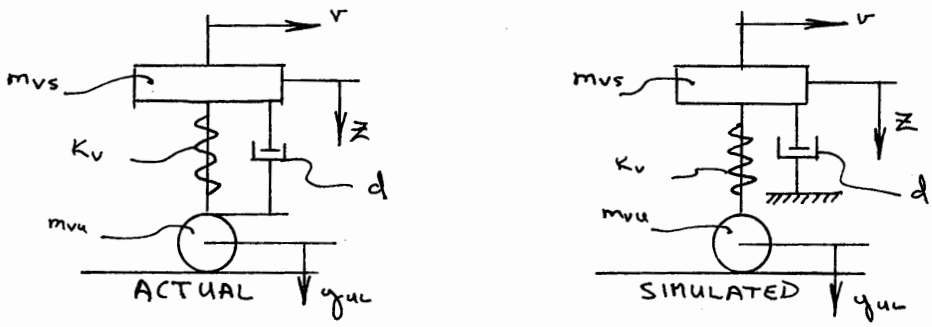

Figure 2. Idealized Vehicle

The spring constant of the vehicle is K_v, and m_{vu} are respectively the sprung and unsprung masses of the vehicle. The equivalent shock absorber is shown as d. The sprung mass may be thought of as the mass carried by the springs while the unsprung mass will include the vehicle's running gear such as wheels, tires, and axles. The velocity of the vehicle is considered constant while it is on the span and is denoted by v. The displacement of the sprung mass is represented by z, which is taken as zero at the static load position. The wheel is assumed to remain in contact with the bridge; therefore, the deflection of the beam, directly under the unsprung mass, is the deflection of the wheel. This deflection is shown as y_{ul}. By summing the vertical dynamic forces, according to the convention used for the beam, the equation for the dynamic equilibrium of the actual vehicle is obtained.

$$m_{vs} \frac{d^2z}{dt^2} + d\left[\frac{d(z - y_{ul})}{dt}\right] + K_v (z - y_{ul}) = 0$$

Because the number of computer elements was limited, the vehicle had to be simplified by assuming the shock absorber was fixed rather than attached to the wheel. This assumption permitted a considerable saving in the amount of computer equipment which would have been required. The dynamic equilibrium of the simulated vehicle is found by summing the vertical dynamic forces.

$$m_{vs} \frac{d^2z}{dt^2} + d \frac{dz}{dt} + K_v (z - y_{ul}) = 0 \quad \ldots\ldots\ldots\ldots \quad (6).$$

Dynamic Force between the Bridge and Vehicle

The force applied to the beam by the vehicle may be considered in two parts. The first is due to the unsprung mass, the second is from the force in the spring. The equations for the forces are,

$$f_1 = m_{vu} \left(g - \frac{d^2 y_{ul}}{d t^2}\right) \quad \ldots\ldots\ldots\ldots\ldots\ldots \quad (7).$$

$$f_2 = K_v (z - y_{ul}) + m_{vs} g \quad \ldots\ldots\ldots\ldots\ldots\ldots \quad (8).$$

$$F = f_1 + f_2 \quad \ldots\ldots\ldots\ldots\ldots\ldots\ldots\ldots \quad (9).$$

Following the sign convention used previously, the equation for the force applied to the beam by the vehicle is

$$F = m_{vu} \left(g - \frac{d^2 y_{ul}}{d t^2}\right) + K_v (z - y_{ul}) + m_{vs} g \quad \ldots\ldots \quad (10).$$

where g is the acceleration due to gravity.

Summary of Equations and Assumptions

For the system shown in figure 3, we now have the following equations:

$$EI \frac{\partial^4 y}{\partial x^4} + m \frac{\partial^2 y}{\partial t^2} + c \frac{\partial y}{\partial t} = m_{vu} \left(g - \frac{d^2 y_{ul}}{d t^2}\right) + K_v (z - y_{ul}) + m_{vs} g \quad (11).$$

$$m_{vs} \frac{d^2 z}{d t^2} + d \frac{d z}{d t} + K_v (z - y_{ul}) = 0 \quad \ldots\ldots\ldots\ldots \quad (12).$$

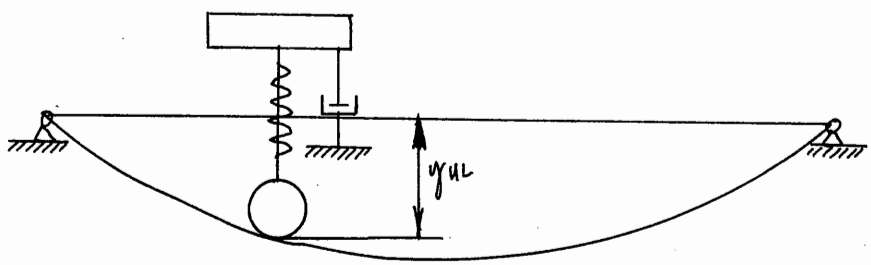

Figure 3. Bridge--Vehicle System

In the derivation of these equations the following assumptions were made:

BEAM

1. The entire bridge system acts as an equivalent single beam whose rigidity corresponds to that of the bridge. This is equivalent to having the vehicle travel directly down the centerline to eliminate any torsional possibilities, and neglecting any differences of deflection between the girders due to actual proximity to the load.
2. The change in the moment of inertia of the girders due to cover plates was neglected. The moment of inertia at the center section was assumed constant for the entire beam.
3. Structural damping is considered equivalent to an appropriate viscous damping.

VEHICLE

1. The multiple axle loads of the actual vehicle are idealized by a single wheel load which is considered to act at the center of gravity of the actual vehicle. The individual springs are considered to act as one; thus, the sprung mass of the vehicle has only one degree of freedom, or one mode of vibration.
2. The vehicle maintains a constant velocity during passage over the span, and the wheel remains in contact with the bridge.

IV

PREPARATION OF EQUATIONS FOR SOLUTION BY ANALOG COMPUTER

Requirements of the Analog Computer

The analog computer consists of a number of high gain amplifiers with the necessary peripheral equipment for operation. Because of the electrical characteristics of the amplifiers, their output is the time integral of the input. Thus, the amplifier is, in essence, an integrator. Feeding the first derivative of a function into the integrator will result in the function as the output. It is this capability of integration that makes it advantageous to use the analog computer for the solution of differential equations.

In the case of a partial differential equation there are several independant variables which must be considered. The computer is capable of integrating only with respect to time. For an ordinary differential equation this is adequate, in that time may be used to represent the single variable. However, for a partial differential equation some means must be employed to reduce the number of independent variables to one, before the solution may be obtained. The technique of finite differences is used in this solution. Dividing the beam into a number of points and applying finite differences at each point to the partial differential equation results in an ordinary differential equation at each point. Each of these equations may now be solved simultaneously with the others.

Solution for Beam

Considering any function, such as shown below, it is possible to obtain the following basic finite difference relationships.

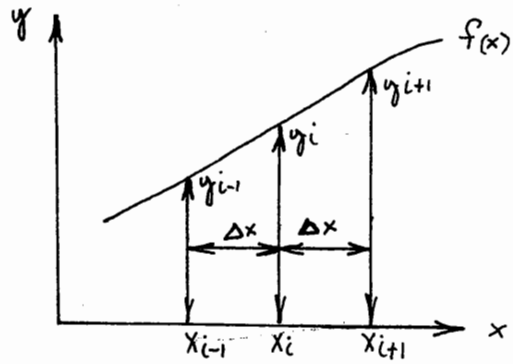

Figure 4. Finite Differences

$$y_i = \frac{y_{i+1} - y_{i-1}}{2} \quad \ldots\ldots\ldots\ldots\ldots\ldots\ldots\ldots (13.a).$$

$$\frac{dy_i}{dx} = \frac{y_{i+1} - y_{i-1}}{2\Delta x} \quad \ldots\ldots\ldots\ldots\ldots\ldots\ldots\ldots (13.b).$$

$$\frac{d^2y_i}{dx^2} = \frac{y_{i+1} - 2y_i + y_{i+1}}{\Delta x^2} \quad \ldots\ldots\ldots\ldots\ldots\ldots (13.c).$$

For a simply supported beam such as shown in figure 5, the following boundary conditions are evident:

$$y_{x=0} = 0 \qquad y_{x=L} = 0$$

$$M_{x=0} = 0 = -EI \frac{d^2y}{dx^2} \qquad M_{x=L} = 0 = -EI \frac{d^2y}{dx^2}$$

The beam is segmented as shown on the diagram with the following boundary conditions:

$$y_o = 0 \qquad y_6 = 0$$

$$M_o = 0 \qquad M_6 = 0$$

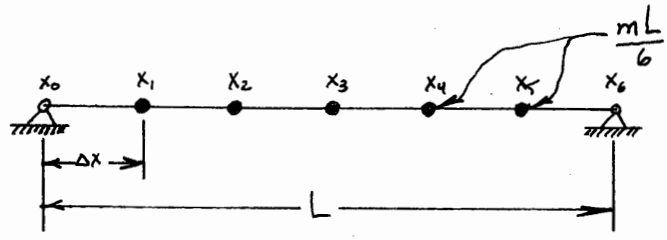

Figure 5. Segmented Beam

Rearranging equation (5) and using equation (2) results in,

$$\frac{\partial^2 y}{\partial t^2} = -\frac{c}{m}\frac{\partial y}{\partial t} + \frac{1}{m}\frac{\partial^2 (M)}{\partial x^2} + \frac{F(t,x)}{m} \quad \ldots\ldots\ldots\ldots (14).$$

The first term on the right side of equation (14) represents the effect of damping, the second term represents the effect of free vibration, and the third term represents the external force applied to the beam. Rewriting equation (14) at point 1, using finite differences for the second derivative of M, and considering only dampened, free vibration by neglecting the third term, we have

$$\frac{d^2 y_1}{dt^2} = \frac{1}{m}\left[\frac{M_0 - 2M_1 + M_2}{\Delta x^2}\right] - \frac{c}{m}\frac{dy_1}{dt}$$

with $x = \frac{L}{6}$, $x^2 = \frac{L^2}{36}$, and $M_0 = 0$

this is

$$\frac{d^2 y_1}{dt^2} = \frac{36}{mL^2}\left[-2M_1 + M_2\right] - \frac{c}{m}\frac{dy_1}{dt} \quad \ldots\ldots\ldots\ldots (15.a).$$

Similarly,

$$\frac{d^2 y_2}{dt^2} = \frac{36}{mL^2}\left[M_1 - 2M_2 + M_3\right] - \frac{c}{m}\frac{dy_2}{dt} \quad \ldots\ldots\ldots\ldots (15.b).$$

$$\frac{d^2 y_3}{dt^2} = \frac{36}{mL^2}\left[M_2 - 2M_3 + M_4\right] - \frac{c}{m}\frac{dy_3}{dt} \quad \ldots\ldots\ldots\ldots (15.c).$$

$$\frac{d^2y_4}{dt^2} = \frac{36}{mL^2}\left[M_3 - 2M_4 + M_5\right] - \frac{c}{m}\frac{dy_4}{dt} \quad \ldots\ldots\ldots\ldots (15.d).$$

$$\frac{d^2y_5}{dt^2} = \frac{36}{mL^2}\left[M_4 - 2M_5\right] - \frac{c}{m}\frac{dy_5}{dt} \quad \ldots\ldots\ldots\ldots\ldots (15.e).$$

Writing finite difference equations for $M = -EI\frac{d^2y}{dt^2}$ at each point with $y_o = 0$, and $y_6 = 0$ results in,

$$M_1 = \frac{-36EI}{L^2}\left[-2y_1 + y_2\right] \quad \ldots\ldots\ldots\ldots\ldots\ldots (16.a).$$

$$M_2 = \frac{-36EI}{L^2}\left[y_1 - 2y_2 + y_3\right] \quad \ldots\ldots\ldots\ldots\ldots (16.b).$$

$$M_3 = \frac{-36EI}{L^2}\left[y_2 - 2y_3 + y_4\right] \quad \ldots\ldots\ldots\ldots\ldots (16.c).$$

$$M_4 = \frac{-36EI}{L^2}\left[y_3 - 2y_4 + y_5\right] \quad \ldots\ldots\ldots\ldots\ldots (16.d).$$

$$M_5 = \frac{-36EI}{L^2}\left[y_4 - 2y_5\right] \quad \ldots\ldots\ldots\ldots\ldots\ldots (16.e).$$

Back substituting these values of M_i into the equation for $\frac{d^2y_i}{dt^2}$ results in the following ordinary differential equations. At point 1

$$\frac{d^2y_1}{dt^2} = \left(\frac{36}{mL^2}\right)\left(\frac{-36EI}{L^2}\right)\left[+5y_1 - 4y_2 + y_3\right] - \frac{c}{m}\frac{dy_1}{dt}$$

or

$$\frac{d^2y_1}{dt^2} = \frac{-1296\ EI}{mL^4}\left[+5y_1 - 4y_2 + y_3\right] - \frac{c}{m}\frac{dy_1}{dt} \quad \ldots\ldots(17.a).$$

Similarly,

$$\frac{d^2y_2}{dt^2} = \frac{-1296\ EI}{mL^4}\left[-4y_1 + 6y_2 - 4y_3 + y_4\right] - \frac{c}{m}\frac{dy_2}{dt} \quad .(17.b).$$

$$\frac{d^2y_3}{dt^2} = \frac{-1296\ EI}{mL^4}\left[y_1 - 4y_2 + 6y_3 - 4y_4 + y_5\right] - \frac{c}{m}\frac{dy_3}{dt} \quad .(17.c).$$

$$\frac{d^2y_4}{dt^2} = \frac{-1296\ EI}{mL^4}\left[y_2 - 4y_3 + 6y_4 - 4y_5\right] - \frac{c}{m}\frac{dy_4}{dt} \quad ..(17.d).$$

$$\frac{d^2y_5}{dt^2} = \frac{-1296\ EI}{mL^4}\left[y_3 - 4y_4 + 5y_5\right] - \frac{c}{m}\frac{dy_5}{dt} \quad \ldots\ldots(17.e).$$

These five ordinary differential equations involve five unknowns, consequently they may be solved simultaneously to obtain the free vibration* solution. The basic circuit diagram for this solution is shown later in figure 6. In this diagram the symbol I.C. represents the initial condition which is applied to the intergrator before the solution begins. By adjusting the potentiometer to vary the value of these initial conditions, it is possible to prescribe the initial deflection of the beam.

Moment at Midspan

In order to obtain the circuit for the moment at the middle of the beam, at point 3, equation (16.c) is used. The moment is simply the sum of the deflections of the point in question and the adjacent points. A circuit for the centerline moment is shown in figure 7.

* For free vibration, c = 0.

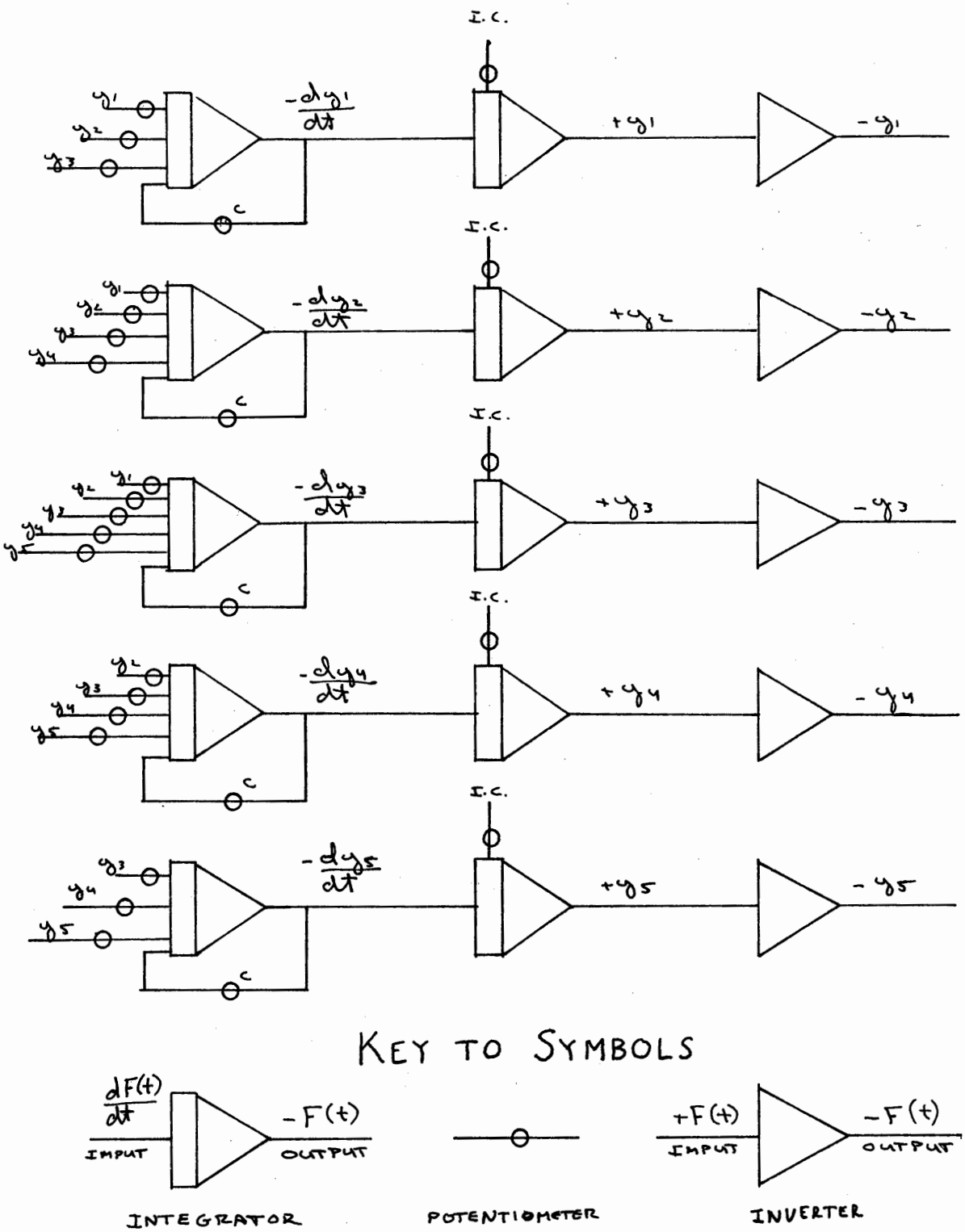

Figure 6. Finite Difference Circuit

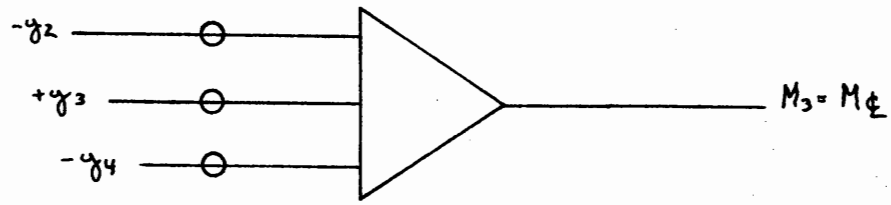

Figure 7. Circuit for Centerline Moment

Solution for Vehicle

Equation (6), the differential equation for the dynamic equilibrium of the vehicle, may be rearranged as follows,

$$\frac{d^2z}{dt^2} = -d'\frac{dz}{dt} - \frac{K_v z}{m_{vs}} + \frac{K_v}{m_{vs}} y_{ul} \quad \ldots\ldots\ldots\ldots (18).$$

where $d' = \frac{1}{m_{vs}} d$.

With the equation in this form it is possible to draw the circuit diagram required to produce it. The circuit is shown in figure 8, below.

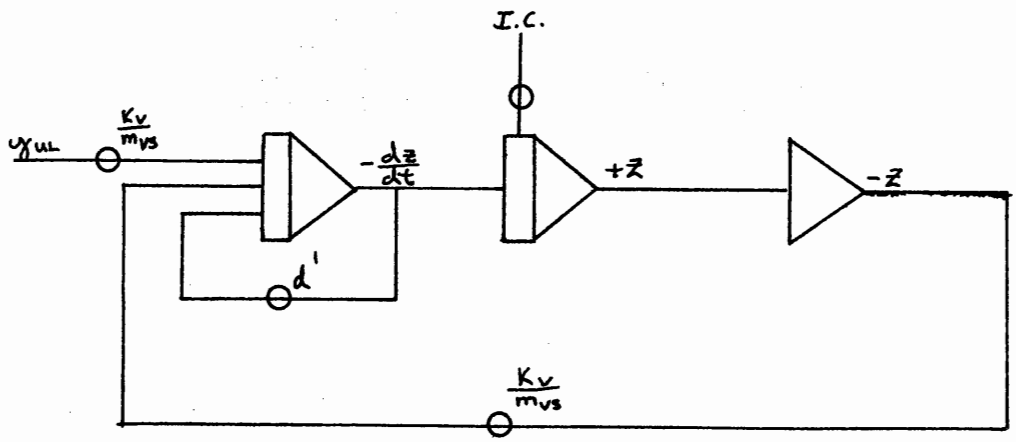

Figure 8. Circuit Diagram for Vehicle

Varying the I.C. in this case is equivalent to starting the vehicle with the spring either compressed or extended. If the approach slab

were below the level of the bridge, the spring would begin in the compressed condition; conversely, if the approach slab were above the level of the bridge, the spring would be extended. A glance at equation (10) indicates that the force applied to the beam increases when the spring is compressed and is reduced when the spring is extended.

Forcing Functions

The basic equations used in this problem are in terms of a continuous variable along the length of the span. However, when reducing the partial differential equation to a set of simultaneous regular differential equations the distance variable is taken at only the discrete points at which the finite difference equations were applied. In order to evaluate the magnitude of quantities at other than the known points, which is required by the equation for the vehicle's equilibrium and force, it is necessary to assume a function relating the known effects to the rest of the beam. It is also necessary to assume a function which will locate the vehicle and apply the force, due to the vehicle, at the points required by its position. Because the velocity of the vehicle is assumed constant, it is possible to relate its position to a function of time.

Five time dependent functions are used to satisfy these requirements. Each is a triangular pulse function, with the peak value obtained at the time when the vehicle is directly over the respective point. The function is zero up to the time when the vehicle reaches the preceding point and then increases linearly up to the next point. These functions are shown graphically on the next page.

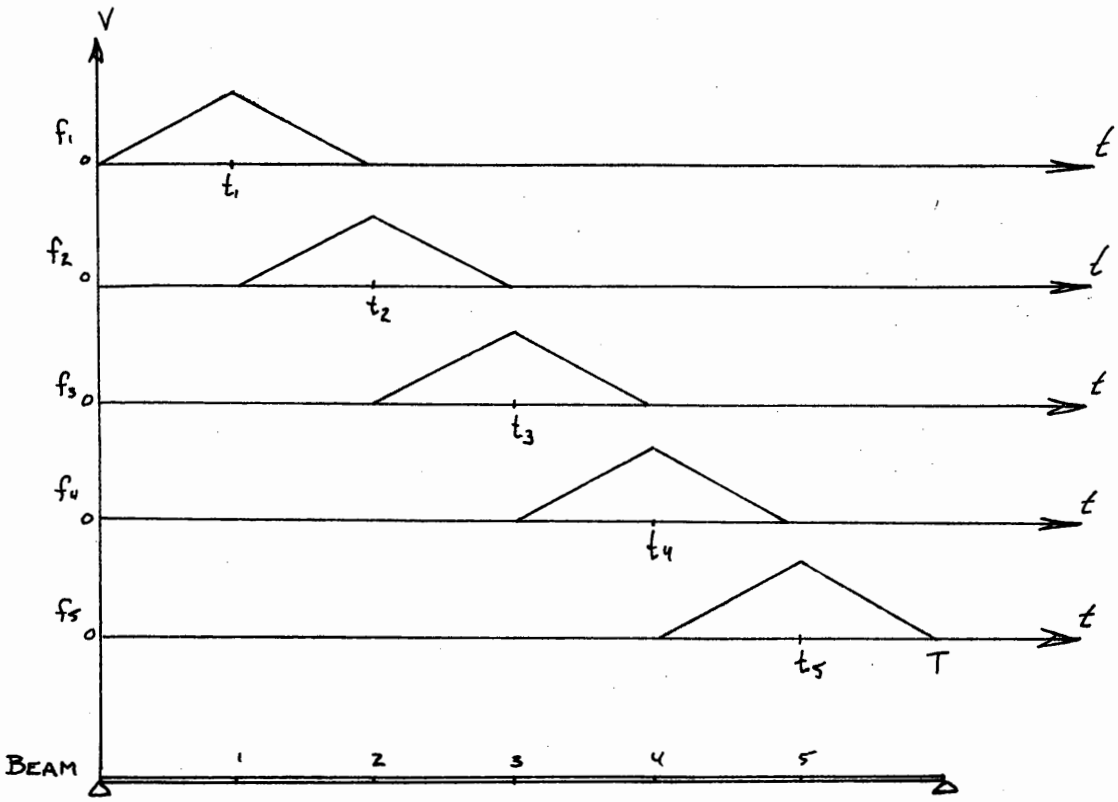

Figure 9. Forcing Functions

Since the time integral of a constant is a line with a constant slope, a typical circuit used to generate one of these functions is shown in figure10. Initially, switch SW1 is open and remains open until the vehicle reaches the prior point. At this point, switch SW1 closes and the voltage passes through switch SW2, which remains closed until the vehicle reaches the point beyond that under consideration. This voltage drivesintegrator 01 which has an output as shown in figure 10. At the same time the voltage passes through a potentiometer into the 10 gain of inverter 02 which then has an output of -2V. Due to the initial condition enforced on integrator 03 this -2V input produces an output which is displaced from the origin, and has a slope twice that of the output of 01, as shown in figure 11.

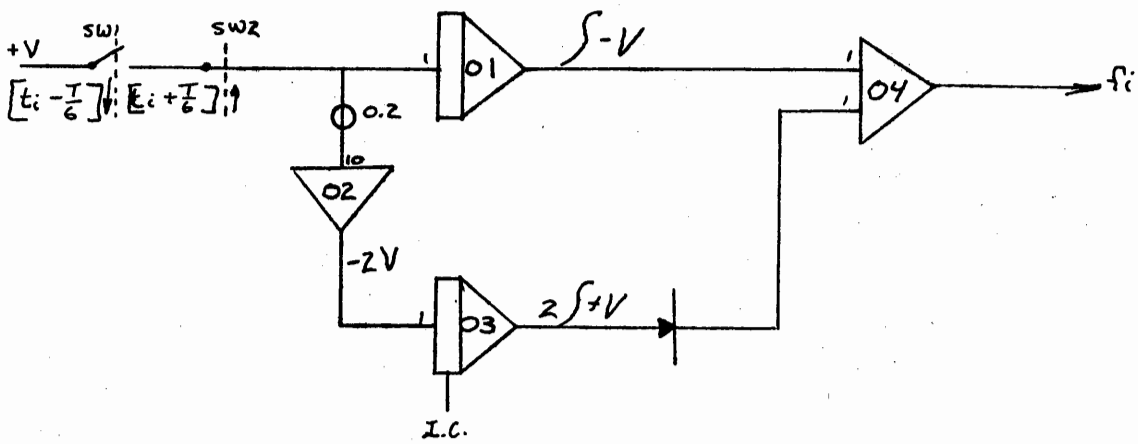

Figure 10. Circuit for a Forcing Function

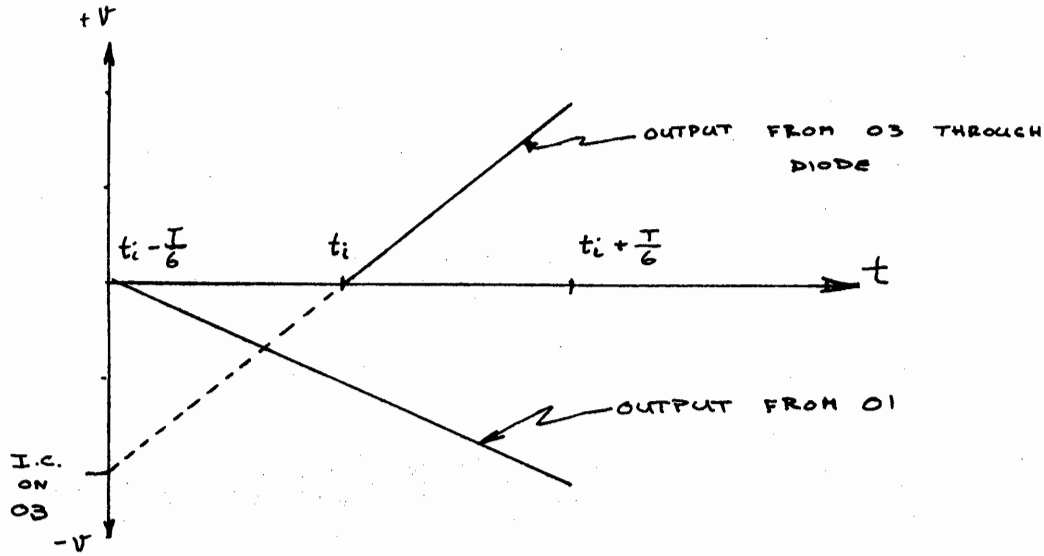

Figure 11. Operation of a Forcing Function Circuit

The output of 03 passes through a diode represented by the symbol  . A diode may be thought of as a switch which passes only positive or only negative voltages. In this configuration it will pass only positive voltages. Thus, the sumer 04 receives only the voltages shown by solid lines in the figure above. The output of 04 from time

$t_i - \frac{T}{6}$ to t_i is the negative of the output of 01, and from then on is the negative of the sum of the outputs of 01 and 04. At time equal to $t_i - \frac{T}{6}$ switch SW2 opens to stop the function. Now the output of 04 is the desired function as shown in figure 12 below. By arranging sets of circuits as explained above, coupled by switches which are activated at the appropriate times, it is possible to generate the desired set of functions.

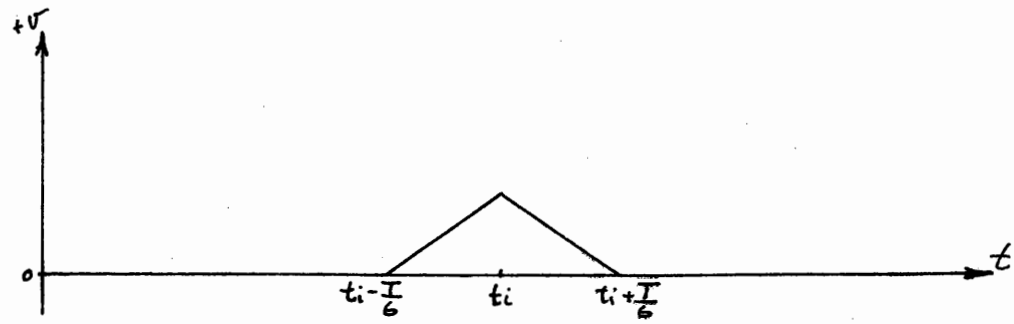

Figure 12. Output of Forcing Function Circuit

In order to evaluate properties at other than known points the function is used in the following manner. Suppose the vehicle is between points 1 and 2, and the value of the deflection of the beam, y, is desired. Consider the values of function 1 and 2, which are the only ones with values between these two points. When the vehicle is directly over point 1, the desired deflection is y_1, which may be obtained by multiplying y_1 by f_1, whose value at that point is unity. When the vehicle is over point 2, the desired deflection is that of y_2. This may be obtained by multiplying y_2 by f_2, which is y_2 at point 2 because f_2 is unity there. By assuming a linear relationship for the deflection, the intermediate points may be found by summing the products of the deflection of each point and its respective function. Thus, midway

between points 1 and 2 the deflection is one-half of y_1 plus one-half of y_2. Since f_1 and f_2 are both equal to one-half at this point, the sum of these products will be the deflection of the point. By similar arguments this product is seen to be the deflection under the load for all other intermediate points. Noting that the individual functions have zero values when the load is beyond the range of influence, it is possible to express y_{ul}, the deflection under the load, as

$$y_{ul} = \sum_{i=1}^{5} y_i f_i \quad \ldots\ldots\ldots\ldots\ldots\ldots\ldots\ldots\ldots\ldots (19).$$

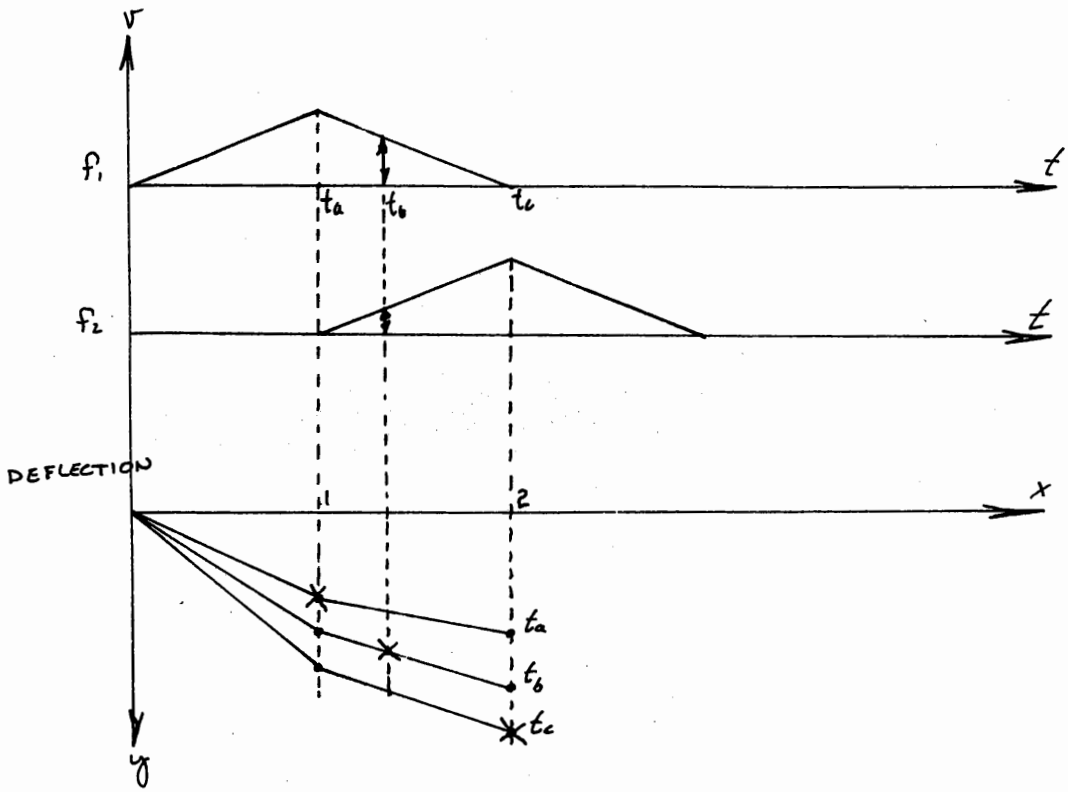

Figure 13. Properties at Intermediate Points

Obviously the acceleration of the beam under the load may be found in the same manner.

$$\frac{d^2y_{ul}}{dt^2} = \sum_{i=1}^{5} \frac{d^2y_i}{dt^2} \quad f_i \quad \ldots\ldots\ldots\ldots\ldots\ldots\ldots (20).$$

Solution for Force

Equation 10, the expression for the force applied to the beam, by the vehicle may be rearranged to

$$F = K_v z - m_{vu} \frac{d^2y_{ul}}{dt^2} - K_v y_{ul} + m_{vt} g \quad \ldots\ldots\ldots\ldots (21),$$

where $m_{vt} = m_{vs} + m_{vu}$. From this equation, the circuit required to produce this force is as shown in figure 14. In order to apply this force to the points along the beam, for the complete solution of the differential equations, it is necessary to multiply the force by each point's respective function before adding it to the circuit for free vibration.

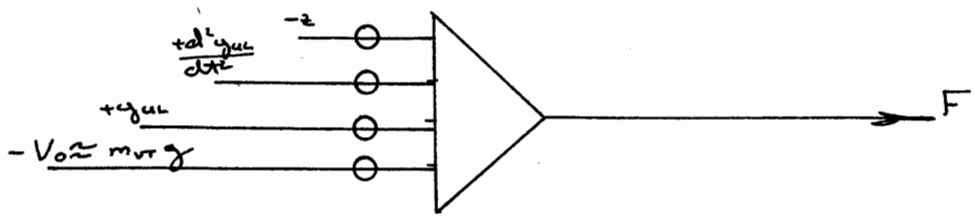

Figure 14. Circuit for Force between Vehicle and Beam

A block diagram for the interconnection of the various elements to form the entire analogy is shown in figure 15. Details of the program for simulation are given in the appendix.

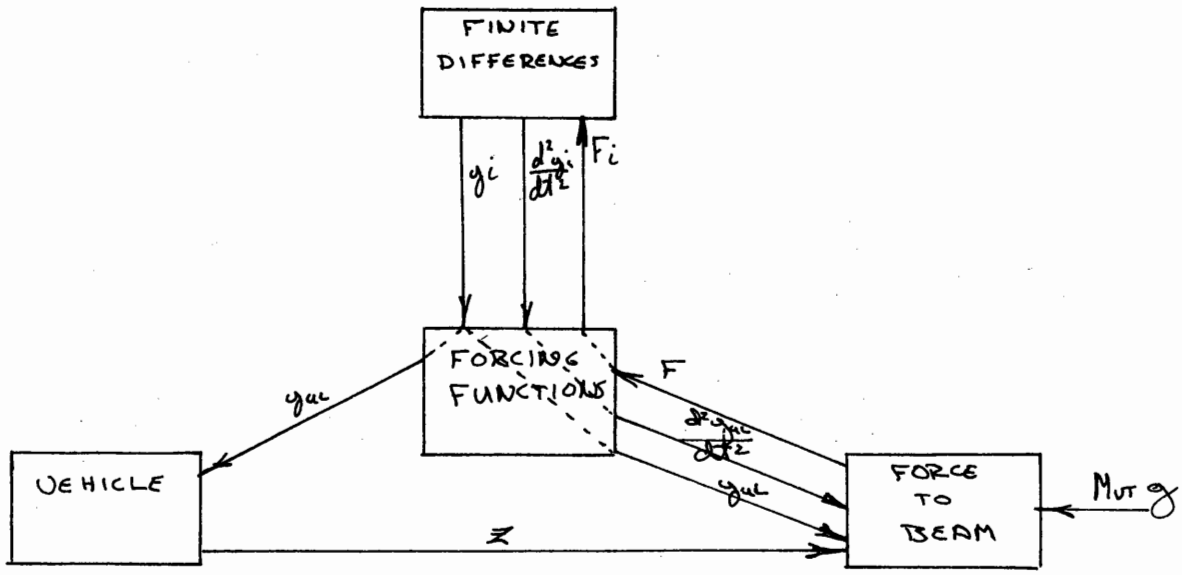

Figure 15. Block Diagram of Analogy

Description of Bridge and Typical Vehicle

The bridge over Ceder Street on I 95 in Branford, Connecticut was chosen to represent a typical single span bridge to be simulated. The span is 90'-0" and consists of two seperate but adjacent spans each carrying two lanes of traffic. Each bridge is 51'-10" wide and includes a 13' raised median, two 12' traffic lanes and a shoulder lane. The bridges are of composite design with welded plate girders. The live load used for design was H20-S16-44.

Properties of the bridge needed to scale the analogy are listed in the appendix along with calculations required. Data reguired for these calculations was obtained directly from the blueprints of the bridge provided by the State Highway Department.

The characteristics of the vehicle were determined from the specifications published by five truck manufacturers. A vehicle, representative of the majority of traffic was the objective. Details of the vehicle simulated are given in the appendix.

V

VERIFICATION OF COMPUTER RESULTS

Individual Circuits

In order to prepare an analogous circuit for the computer, the operator connects the various circuit elements by means of a large patch board. The elements are connected by plug-in leads which are inserted into the board in various positions depending upon the element and configuration desired. In this manner the circuit may be removed from the computer, permitting work on a different circuit, by removing the first patch board and replacing it with another.

In the process of constructing this analogy the patching was done in steps corresponding to the different sections of the model. The first step was the circuit to solve the equation for solution of the free vibration of an unloaded beam. The second step was the circuit representing the free vibration of the vehicle and the third step was the generation of the forcing functions. As each step was completed, the analogy was verified, prior to the interconnection.

The section corresponding to the free vibration of the beam was first checked with the damping coefficients equal to zero. The beam was given an initial deflection corresponding to the mode shapes of the first four natural frequencies. The subsequent deflection output of each point for the vibration from this position was plotted on the eight channel recorder used throughout this study. The recording was

then scaled to determine the frequency and mode shape of the output to evaluate the response, which was found to be in very close agreement with analytical predictions.

To prevent this circuit from becoming unstable or regenerative, the damping influence had to be included. The damping characteristics of a bridge are a particularly elusive property in view of the complex nature of material damping (3). However, this difficulty was bypassed by assuming an equivalent viscous damping. From experimental results obtained on similar bridges (4), it was found that the amplitude of the tenth cycle of free vibration was about 60 percent of the initial amplitude. By adjusting the potentiometers corresponding to the coefficients of viscous damping during free vibration, caused by imposed initial conditions; the analogy was made to respond in this way.

A similar procedure was used in checking the circuit representing the free vibration of the vehicle. The sprung mass was given an initial deflection and the undampened response was compared with the analytically expected response. The damping coefficient was then adjusted to provide a dampened response similar to that of a typical vehicle (1). Tracings of typical outputs of the deflection of the beam and vehicle in both dampened and undampened states are shown in figure 16.

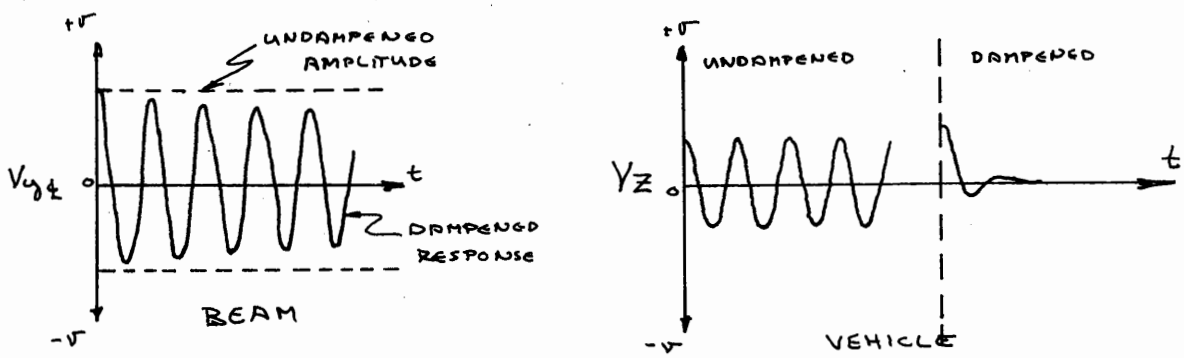

Figure 16. Typical Unloaded Response of Beam and Vehicle

Solution for a Beam under a Constant Force

When the forcing functions were operating properly, the different sections were interconnected. A detailed circuit diagram of the entire analogy is included in the appendix. As a check of the computer results, the vehicle was replaced by a constant force traveling across the beam at a constant velocity. The analytical solution for this problem has been discussed by a number of authors (5,6), including Biggs (4), who gives the following equation for the first mode deflection of an undampened, simply supported beam under the influence of a constant force traveling with a constant velocity;

$$y = \frac{2F}{mL}\left(\frac{1}{w^2 - \Omega^2}\right)\left[\operatorname{Sin}\Omega t - \frac{\Omega}{w}\operatorname{Sin} wt\right] \operatorname{Sin}\frac{\pi x}{L} \quad \ldots\ldots(22).$$

where

F = magnitude of force

m = mass of beam per unit length

L = length of span

w = fundamental frequency of beam $\left(\sqrt{\frac{EI}{L}}\right)$

$\Omega = \frac{\pi V}{L}$ where V is the velocity of the vehicle

t = time (t = 0, when force starts on beam)

x = distance along beam

Differentiating equation (22) with respect to time results in

$$\frac{\partial y}{\partial t} = \frac{2F}{mL}\left(\frac{1}{w^2 - \Omega^2}\right)\left[\Omega\cos\Omega t - \Omega \cos wt\right] \sin\frac{\pi x}{L} \ldots(23).$$

Using these equations the mid-span deflection, when the force is at

mid span, and the maximum amplitude of free vibration may be determined analytically. The analytical results may then be compared with the results obtained by the computer.

Mid-Span Deflection with Force at Centerline

At the centerline $x = \frac{L}{2}$, therefore the last term in equations (22) and (23), $\sin \frac{\pi x}{L}$, is equal to unity. The time at which the force leaves the span may be denoted as t_F, which is equal to $\frac{L}{V}$. When the force is at the centerline, t will be equal to $\frac{t_F}{2}$ and $\sin \Omega t$ may be written as $\sin \frac{\pi V}{L} \cdot \frac{L}{2V}$ or $\sin \frac{\pi}{2}$ which is also equal to unity. Our basic equations are now

$$y_{t=\frac{t_F}{2}} = \frac{2F}{mL}\left(\frac{1}{w^2 - \Omega^2}\right)\left[1 - \frac{\Omega}{w} \sin \frac{wt_F}{2}\right] \quad \ldots\ldots\ldots (24).$$

Deflections computed using this equation at different velocities are tabulated in the appendix, and shown graphically in comparison with the computer results in figure 17.

Maximum Mid-Span Deflection during Free Vibration

If we know the time when the force leaves the span and the mid-span point, equations (22) and (23) become

$$y_{t=t_F} = \frac{2F}{mL}\left(\frac{1}{w^2 - \Omega^2}\right)\left[-\frac{\Omega}{w} \sin wt_F\right] \quad \ldots\ldots\ldots (25).$$

$$\frac{dy}{dt}_{t=t_F} = \frac{2F}{mL}\left(\frac{\Omega}{w^2 - \Omega^2}\right)\left[1 - \cos wt_F\right] \quad \ldots\ldots\ldots (26).$$

These equations represent the initial conditions of the subsequent

free vibration. The equation for the undampened free vibration of the beam in these terms is

$$y_{\ell} = \frac{d y_{\ell, t_F}}{d t} \frac{1}{w} \sin wt' - y_{\ell,\ t_F} \cos wt' \quad \ldots(27).$$

where $t' = 0$ when $t = t_F$.

Substituting equations (25) and (26) into equation (27) and expanding results in

$$y_{\ell} = \frac{2F}{mL}\left(\frac{1}{w^2 - \Omega^2}\right)\left(\frac{\Omega}{w}\right)\left[\sin wt' - \cos wt_F \sin wt' - \sin wt_F \cos wt'\right] \quad (28).$$

Making use of the following trigonometric identities we are able to reduce equation (28) to

$$\sin A \cos B = \frac{1}{2}\left[\sin (A + B) + \sin (A - B)\right]$$

$$\cos A \sin B = \frac{1}{2}\left[\sin (A + B) - \sin (A - B)\right]$$

$$y_{\ell} = \frac{2F}{mL}\left(\frac{1}{w^2 - \Omega^2}\right)\left(\frac{\Omega}{w}\right)\left[\sin wt' - \sin (wt_F + wt')\right] \quad \ldots(29).$$

By finding the derivative of equation (29) with respect to time and setting it equal to zero, we may solve for the time at which the maximum amplitude will occur.

$$\frac{d y}{d t}_{\ell} = 0 = \frac{2F}{mL}\left(\frac{1}{w^2 - \Omega^2}\right)\left(\frac{\Omega}{w}\right)\left[w \cos wt' - w \cos (wt_F + wt')\right]. \quad (30).$$

In order for equation (30) to be equal to zero we must have

$$\left[w \cos wt' - w \cos (wt_F + wt') \right] = 0 \quad \ldots\ldots\ldots (31).$$

Using the identity

$$\cos A - \cos B = 2 \sin \frac{1}{2} (A + B) \sin \frac{1}{2} (B - A)$$

we may rewrite equation (31) as

$$2 \sin \left(wt' + \frac{wt_F}{2}\right) \sin \frac{wt_F}{2} = 0 \quad \ldots\ldots\ldots\ldots (32).$$

To solve equation (32) we have two possibilities. In the first case the equation will be satisfied if

$$\frac{wt_F}{2} = n\pi,$$

however this represents the resonant condition which is beyond the range of physical variables considered in this study. The second possibility is that

$$wt' - \frac{wt_F}{2} = n\pi .$$

Therefore, the time at which the maximum deflection occurs, during free vibration, may be condidered as

$$t'_{max.} = \frac{n\pi}{w} - \frac{t_F}{2} \quad \ldots\ldots\ldots\ldots\ldots\ldots\ldots (33).$$

Substituting this value for time, back into equation (29), we have the solution for the maximum mid-span deflection during free vibration.

$$y_{\ell,MAX} = \frac{4F}{mL}\left(\frac{1}{w^2 - \Omega^2}\right)\frac{\Omega}{w}\left(\sin\frac{wt_F}{2}\right) \quad \ldots\ldots\ldots(34).$$

Using this equation the deflections at different velocities were computed. The results are tabulated in the appendix and are shown in figure 17.

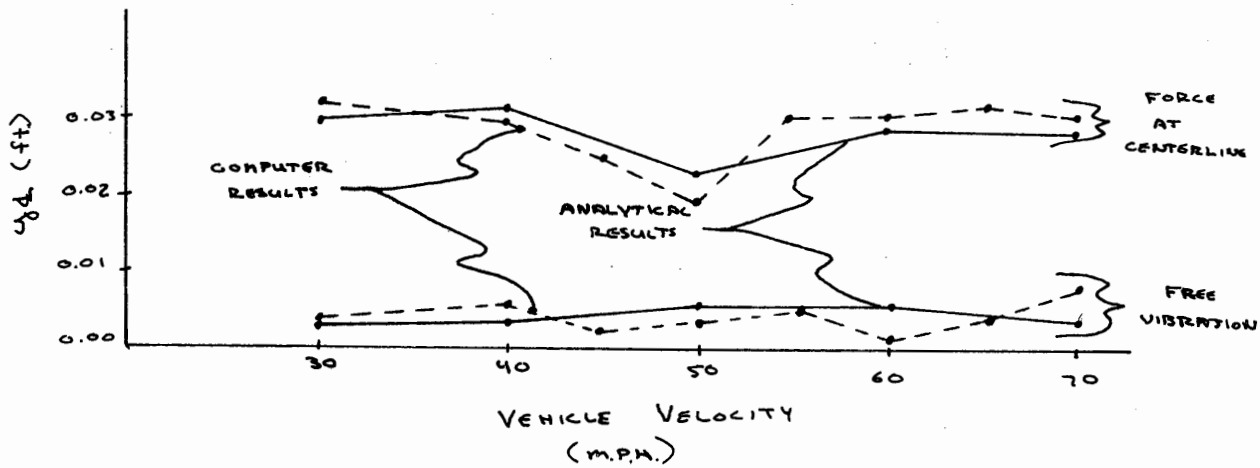

Figure 17. Mid-Span Deflection with Constant Force at Centerline and from Free Vibration due to Constant Force.

"Crawl" Deflections

As an additional verification of the analogy, the velocity of the constant force was reduced. In this manner the deflection and moment at the centerline, plotted against time elapsed or vehicle position would be equivalent to the influence line for deflection or moment at the centerline.

Ideally, the velocity would have been reduced to about 5 m.p.h., but the extent of reduction was restricted by the characteristics of the computer. The optimum duration of each simulation is in the order of one to two minutes. As the length of time required for a simulation is increased, the output becomes less reliable because of ampli-

fier drift and random noise. On the other hand, the response capabilities of the equipment prohibit a decrease in the duration of the simulation.

Because of these restrictions, the circuit was scaled to a range of vehicle speed between 40 m.p.h. and 70 m.p.h.; consequently, the lowest speed which could be utilized with sufficient reliability was 20 m.p.h. However, this was adequate to produce very nearly the results theoretically desired. In this case the influence line for the deflection at the centerline will be a third order curve and a triangular pulse for the moment.

VI

RESULTS

Once the analogy was debugged and adequately verified, simulations were performed to determine the effect of vehicle velocity and fluctuation in the height of the approach slab. The velocity was varied in 10 m.p.h. increments from 40 m.p.h. to 70 m.p.h. The height of the approach slab was taken from 2 inches below the bridge to 1 inch above, in 1 inch increments. Each velocity was set and checked, then an average of three or four runs were made for each appraoch slab height.

The output was listed on the computer's eight channel recorder. Generally, four channels indicated deflection of points including that of the centerline, two channels were used to observe the forcing functions, one for the force between the vehicle and the bridge, and one for the moment at mid span. The recorder had provisions for altering the range of the trace during operation to improve the precision of the values indicated. The maximum negative mid-span deflection and moment was taken from the trace and then averaged with the subsequent results for the same circumstances. Then the approach slab height was altered and the procedure was repeated. After all the heights had been finished, the velocity was changed and the process continued. A reproduction of typical traces of mid-span deflection and moment is shown in figure 18.

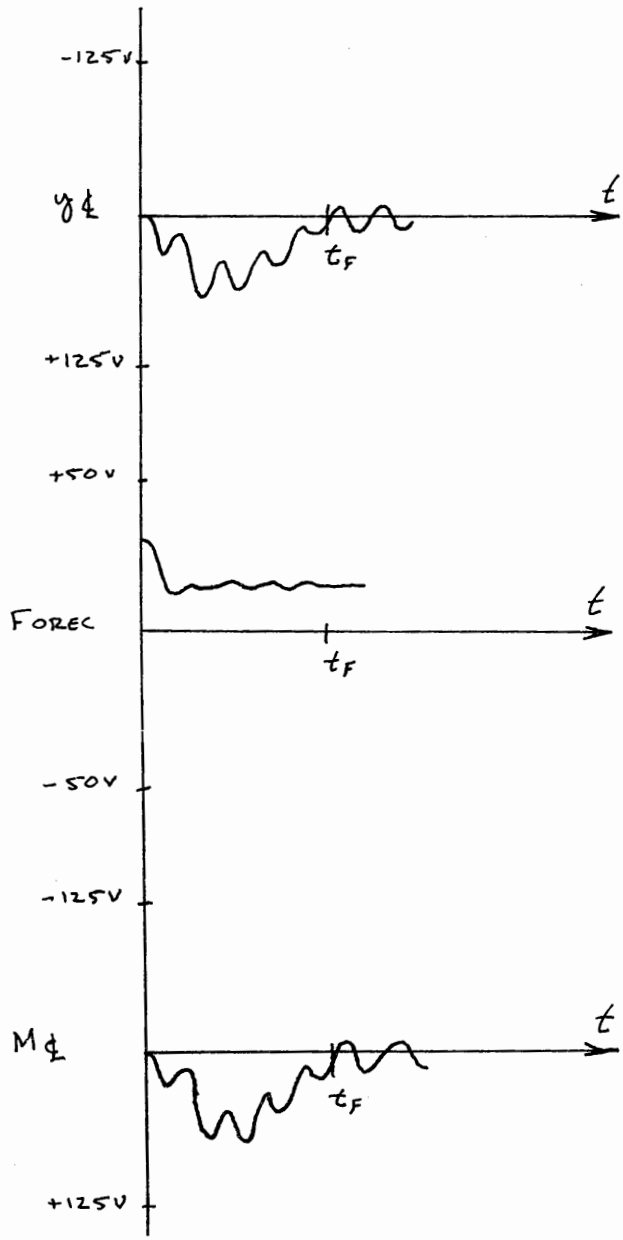

Figure 18. Typical Output

The output obtained from the recorder is in terms of a voltage. This must be converted to the correct units by means of scale factors which were incorporated in the circuit. A tabulation of these scale factors is included in the appendix. Once the average maximum negative moment has been obtained, it is possible to compute the tensile stress induced in the concrete deck using the following equation with the appropriate conversion factors for correspondence of units.

$$\sigma = \frac{nMc}{I}$$

The results may be best shown graphically; thus, figure 19 demonstrates the fluctuation of the variables.

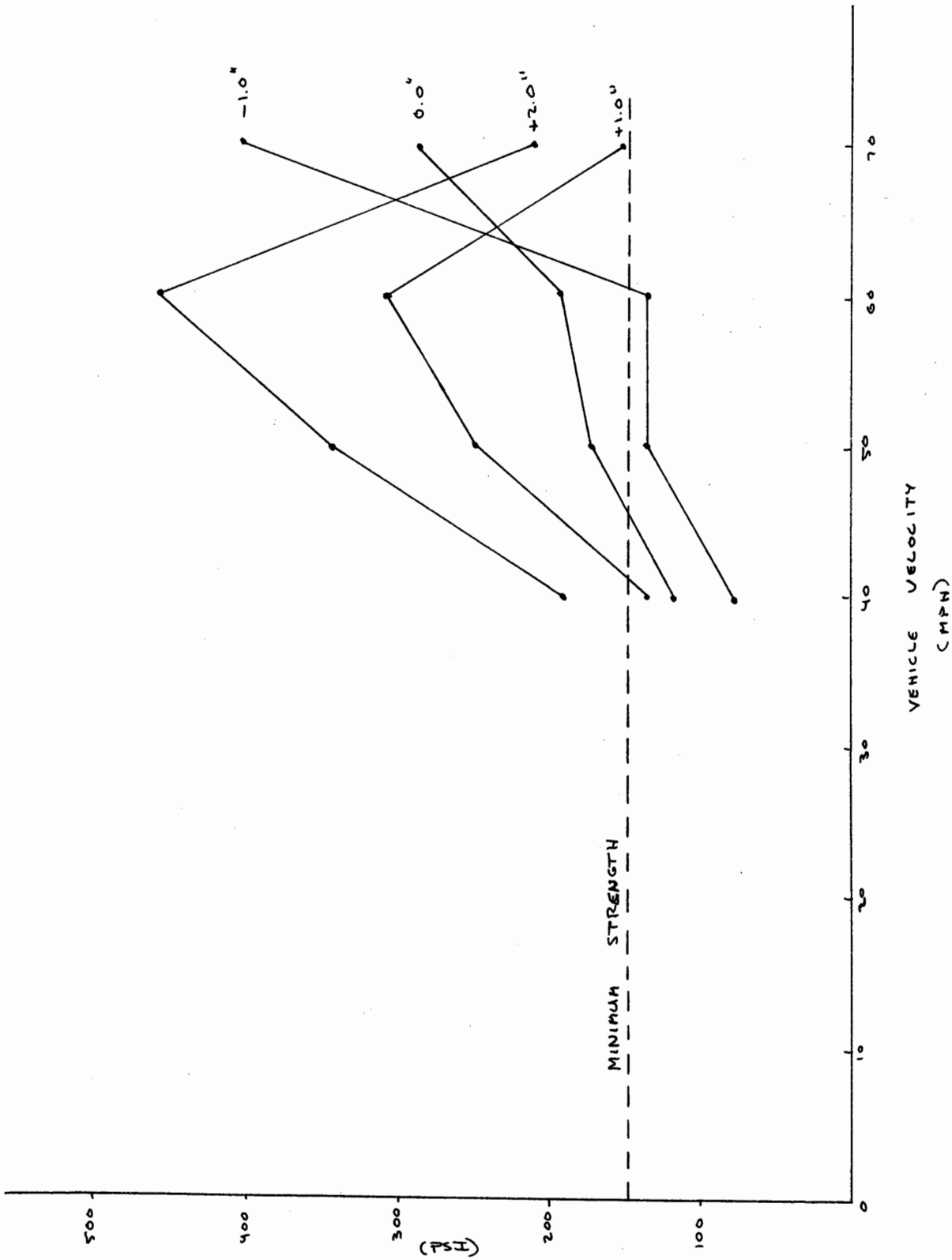

Figure 19. Maximum Tensile Stress in Concrete

VII

CONCLUSION

The possibility of dynamically induced cracks is influenced by the level of stress the material is subjected to and by the strength of the material. The compressive strength of concrete is easily predicted and determined, whereas the tensile strength remains a nebulous and highly variable property. An empirical rule of thumb for static tensile strength permits 10 percent of the static compression strength. For dynamic loading the expected strength is taken as one-half the static strength. Combining these two would indicate a dynamic tensile strength of 5 percent of the static compressive strength.

State specifications require Class "A" Concrete for bridge decks, meaning the minimum static compressive strength will be 3,000 psi. Consequently, a dynamic tensile strength of about 150 psi may be expected. A glance at figure 19, indicates that for the majority of the cases considered this value is less than the stresses computed, indicating a distinct possibility of the presence of dynamically induced cracks.

There are several other factors which must be considered. First the acting composite stiffness of the actual bridge is often higher than the design stiffness. This would reduce the magnitude of the stress induced to the concrete. Second, the static compressive strength of the concrete may well exceed the minimum specified, thus

increasing the dynamic tensile strength proportionally. Third, the fact that actual vehicles have several axles, rather than one wheel, might indicate a reduction in the level of stress, if the rear axle were spaced in such a way as to cancel the effect of the front axle.

In summary, it may be said that the order of magnitude of dynamically induced stress is sufficient to either initiate or aggravate transverse cracks in concrete bridge decks. These cracks will be in the middle section of the span and decreasing in occurrence farther from the centerline of the span.

LIST OF REFERENCES

1. B. S. Cain, Vibration of Rail and Road Vehicles, Pitman Publishing, New York, (1940).

2. R. E. D. Bishop, Vibration, Cambridge University Press, London, (1965).

3. Jerome E. Ruzicka, Structural Damping, The American Society of Mechanical Engineers, New York,(1959).

4. John M. Biggs, Introduction to Structural Dynamics, McGraw-Hill, New York, (1964).

5. C. E. Inglis, A Mathematical Treatise of Vibrations in Railway Bridges, Cambridge University Press, London, (1934).

6. S. Timoshenko, Vibration Problems in Engineering, D. Van Nostrand, New York, (1955).

APPENDIX

Potentiometer Settings

P00	0.5002	P44	0.3333
P01	0.3450	Q01	0.3000
P02	0.2762	Q02	0.6903
P03	1.0002	Q03	0.8667
P04	0.2000	Q04	0.1650
P05	0.8666	Q05	0.0060
P06	0.6901	Q06	0.4142
P07	0.2761	Q07	0.2762
P08	0.0000	Q08	0.5999
P09	0.5003	Q09	0.1001
P10	0.3560	Q10	0.4000
P11	0.4140	Q11	0.6900
P12	0.2763	Q12	0.2760
P13	0.0027	Q13	1.0000
P14	1.0000	Q14	0.2000
P15	1.0000	Q15	0.1003
P17	0.2701	Q16	0.3452
P18	0.2000	Q17	0.2940
P19	0.4000	Q18	0.2002
P20	1.0000	Q19	1.0000
P21	0.6900	Q20	0.4999
P22	0.2762	Q21	0.6900
P23	0.4139	Q22	0.2764
P24	0.0027	Q23	0.4999
P25	0.3560	Q24	0.9995
P26	0.4000	Q25	0.4000
P27	0.2999	Q26	0.0027
P28	0.3003	Q27	0.0027
P29	0.2000	Q29	0.2000
P30	0.0000	Q31	0.1999
P31	0.0000	Q33	0.1000
P32	0.1470	Q34	0.1655
P33	0.0692	Q35	0.7120
P34	0.2000	Q38	0.0300
P35	0.0027	Q39	0.0500
P38	0.2000	Q45	0.1500
P39	0.6900		

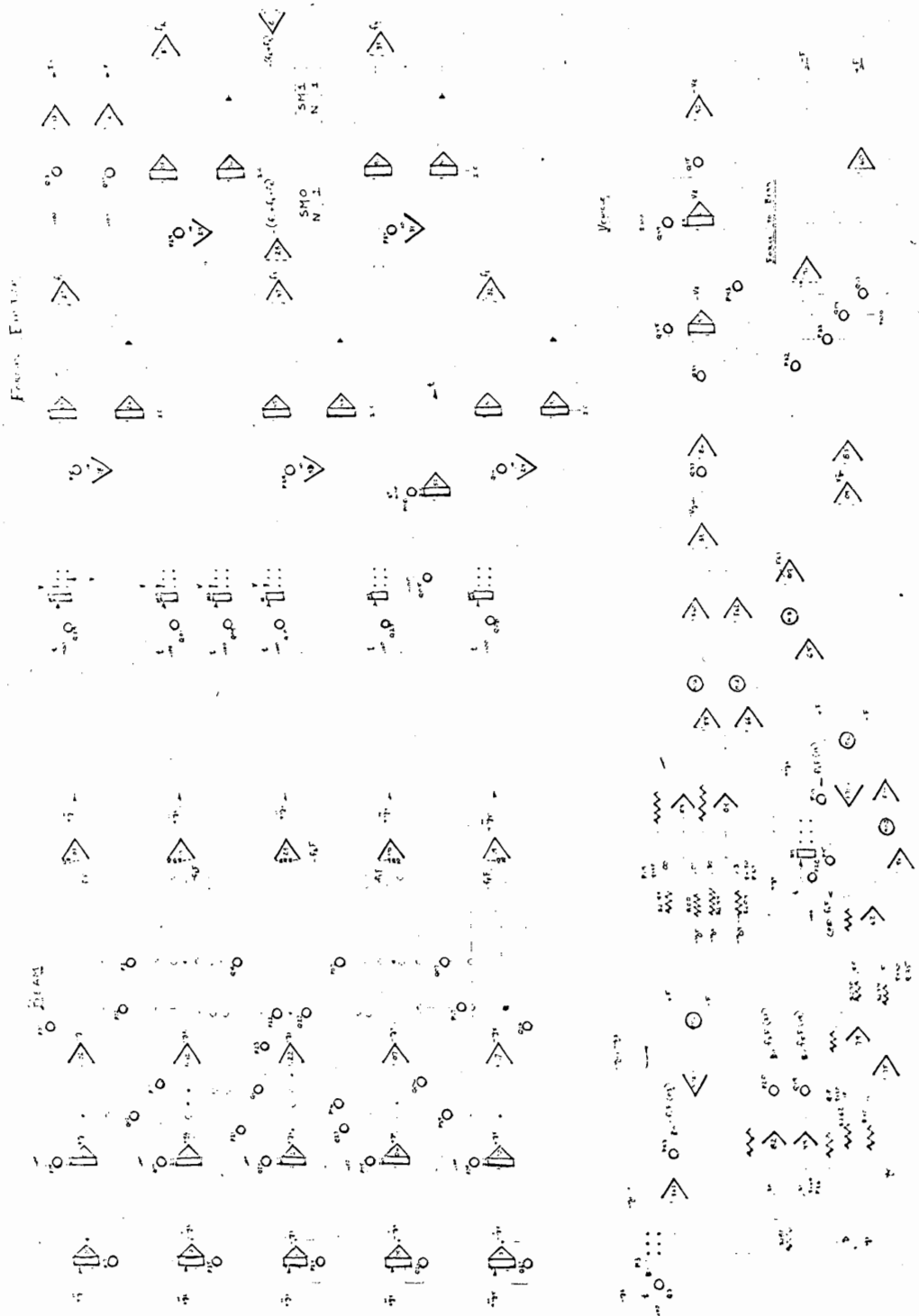

Complete Circuit Diagram

SCALE FACTORS

$$V_y = 2000 \ \frac{\text{volts}}{\text{ft.}}$$

$$V_{\dot{y}} = 20 \ \frac{\text{volts}}{\text{ft./sec.}}$$

$$V_{\ddot{y}} = 0.2 \ \frac{\text{volts}}{\text{ft./sec.}^2}$$

$$V_z = 500 \ \frac{\text{volts}}{\text{ft.}}$$

$$V_{\dot{z}} = 5 \ \frac{\text{volts}}{\text{ft./sec.}}$$

$$V_{\ddot{z}} = 0.05 \ \frac{\text{volts}}{\text{ft./sec.}^2}$$

$$V_F = 2.0 \times 10^{-3} \ \frac{\text{volts}}{\#}$$

$$V_M = 2.22 \times 10^{-5} \ \frac{\text{volts}}{\text{ft. } \#}$$

$$\text{Time Scale} = \frac{1}{100}$$

BRIDGE PROPERTIES

$L = 90'-0"$

Weight = 6635# / linear ft.

m = 207 #mass / linear ft.

$I = 16.75 \text{ ft.}^4$

$w = \frac{EI}{L} = 3.634$ cycles / sec.

VEHICLE PROPERTIES

Simulated vehicle equivalent to fully loaded trucks.

$m_{vu} = 540$ # mass

$m_{vs} = 3460$ # mass

$m_{vt} = 4000$ # mass

$K_v = 1.14 \times 10^6$ # / ft.

TABULATED ANALYTICAL RESULTS

Velocity (mph)	Deflection Force at Mid-Span (ft)	Deflection Free Vibration (ft)
30	0.03008	0.003490
40	0.030173	0.004653
50	0.023227	0.005962
60	0.029773	0.005632
70	0.029116	0.004622

BIBLIOGRAPHY

C. E. Inglis, A Mathematical Treatise of Vibrations in Railway Bridges, Cambridge University Press, London, (1934).

Norris, Hansen, Holley, Biggs, Namyet, Minami, Structural Design for Dynamic Loads, McGraw-Hill, New York, (1959).

Rogers, Connolly, Analog Computation in Engineering Design, McGraw-Hill, New York, (1960).

William W. Seto, Mechanical Vibrations, Schaum, New York, (1964).

Ayre, Ford, Jacobsen, Transverse Vibration of a Two-Span Beam Under Action of a Moving Constant Force, Journal of Applied Mechanics, Vol. 17, (1950).

G. D. McMann, R. H. MacNeal, Beam Vibration Analysis with the Electric-Analog Computer, Journal of Applied Mechanics, Vol. 17, (1950).

James W. Gillespie, Boen-Dar Liaw, Frequency Analysis of Beam by Flexibility Method, Journal of the Applied Mechanics Division, Proceedings of the American Society of Civil Engineers, (February, 1964).

V. H. Heubert, Lumping of Mass in Calculating Vibration Response, Journal of the Applied Mechanics Division, Proceedings of the American Society of Civil Engineers, (February, 1964).

Walter C. Hurty, Vibrations of Structural Systems by Component Mode Synthesis, Journal of the Applied Mechanics Division, Proceedings of the American Society of Civil Engineers, (August, 1960).

Nathan M. Newmark, A Method of Computation for Structural Dynamics, Journal of the Applied Mechanics Division, Proceedings of the American Society of Civil Engineers, (July, 1959).

John F. Fleming, James P. Romualdi, Dynamic Response of Highway Bridges, Journal of the Structural Division, Proceedings of the American Society of Civil Engineers, (October, 1961).

Robert K. Wen, A. S. Veletsos, Dynamic Behavior of Simple Span Highway Bridges, Bulletin 315, Highway Research Board, Washington, (1962).

William Zuk, Bridge Vibrations as Influenced by Elastomeric Bearings, Bulletin 315, Highway Research Board, Washington, (1962).

Dynamic Studies of Bridges on the AASHO Road Test, Special Report #71, Highway Research Board, Washington, (1954).

Vibration and Stresses in Girder Bridges, Bulletin 124, Highway Research Board, Washington, (1956).

W. Brunner, Boundry Value Problems, Princeton Computation Center Report #154, Electronics Associates Inc., Princeton, N.J., (1960).

R. R. Favreau, W. Brunner, Application of the Parameter Influence Coefficient Technique to Boundry Value Problems , Princeton Computation Center Report #156, Electronics Associates Inc., Princeton, N.J., (1960).

Robert M. Howe, Vincent S. Hanemen Jr., The Solution of Partial Differential Equations by Different Methods of Using the Electronic Differential Analyzer, Proceedings of the Institute of Radio Engineers, Pg. 1497, Vol. 412, (1953).